Iranian Journal of Medical Physics
Vol. 12, No. 2, Spring 2015, 129-136
Received: January 18, 2015; Accepted: May 19, 2015

Original Article

Design and Simulation of Photoneutron Source by MCNPX Monte Carlo Code for Boron Neutron Capture Therapy

Mona Zolfaghari[1*], Mahmood Sedaghatizadeh[1]

Abstract

Introduction
Electron linear accelerator (LINAC) can be used for neutron production in Boron Neutron Capture Therapy (BNCT). BNCT is an external radiotherapeutic method for the treatment of some cancers. In this study, Varian 2300 C/D LINAC was simulated as an electron accelerator-based photoneutron source to provide a suitable neutron flux for BNCT.

Materials and Methods
Photoneutron sources were simulated, using MCNPX Monte Carlo code. In this study, a 20 MeV LINAC was utilized for electron-photon reactions. After the evaluation of cross-sections and threshold energies, lead (Pb), uranium (U) and beryllium deuteride (BeD_2) were selected as photoneutron sources.

Results
According to the simulation results, optimized photoneutron sources with a compact volume and photoneutron yields of 10^7, 10^8 and 10^9 ($n.cm^{-2}.s^{-1}$) were obtained for Pb, U and BeD_2 composites. Also, photoneutrons increased by using enriched U (10-60%) as an electron accelerator-based photoneutron source.

Conclusion
Optimized photoneutron sources were obtained with compact sizes of 10^7, 10^8 and 10^9 ($n.cm^{-2}.s^{-1}$), respectively. These fluxs can be applied for BNCT by decelerating fast neutrons and using a suitable beam-shaping assembly, surrounding electron-photon and photoneutron sources.

Keywords: LINAC, BNCT, Fast Neutrons

1- Department of Physics, Faculty of Science, K. N. T University of Technology, Tehran, Iran.
*Corresponding author: Tel: +982123064335, E-mail: m.zolfaghary.8695@gmail.com

1. Introduction

In Boron Neutron Capture Therapy (BNCT), boron 10 (^{10}B), as a stable isotope delivered to tumor tissues, is irradiated by thermal neutrons (E_n<0.1 eV). Neutron capture reactions occur due to the high value of thermal neutron capture cross-section in ^{10}B (3,837 barns). Following the $^{10}B(n, \alpha)^7Li$ reaction, lithium 7 (^7Li) and alpha are produced (^4He and ^7Li with 1.47 and 0.84 MeV energies, respectively). In 93.7% of cases, a 478 keV gamma ray is emitted [1, 2]:

$$^{10}B + n_{th} \longrightarrow [^{11}B] \longrightarrow ^7Li + \alpha + E_\gamma(478keV) + 2.312\ MeV \quad (1)$$

High linear energy transfer (LET) of produced particles in their path lengths in soft tissues (~9 μm for α particle and 5 μm for lithium ion) lead to the destruction of malignant cells by losing their high energy in boron-containing cells [3].

BNCT has been applied for the treatment of high-grade gliomas [1], cerebral metastases [4] and primary cutaneous melanoma [5]. Most recently, the application of this modality has extended to head, neck and liver cancers. Neutron sources in BNCT include nuclear reactors, as well as proton and deuteron accelerators, based on $^7Li(p, n)^7Be$ and $^9Be(d, n)^{10}B$ reactions and ^{252}Cf [6]. Also, electron accelerator-based photoneutron sources can be used in BNCT via generating thermal and epithermal neutron beams; these sources are suitable for BNCT application at hospitals [7].

Photons are produced when high-energy electrons impact a (e, γ) target. For heavy nuclei (A> 150), photon absorption leads to neutron emission. The cross-section value of this process is at its maximum level with a photon energy range of 13-18 MeV for heavy nuclei and 20-23 MeV for light nuclei (A< 40). Overall, beryllium (Be) and deuteride (D) have been shown to have 1.67 and 2.23 MeV energies, respectively [8].

Electron linear accelerators (LINAC) with high energy (18-25 MeV) can be a source of photoneutrons, which are produced by giant dipole resonance reactions [9]. In 2006, researchers in Italy used a small-sized LINAC-based neutron source with a flux rate of 10^6 ($n.cm^{-2}.s^{-1}$). The optimized neutron source (called PhoNeS) created a neutron flux of 10^8 ($n.cm^{-2}.s^{-1}$) [10]. Moreover, in 2009, patients with lung cancer were treated after boronophenylalanine administration with neutron beams, using PhoNeS. The treatment results were reported to be satisfactory [12].

It should be noted that photoneutron sources produce fast neutrons, which cannot be directly used in BNCT. Therefore, a beam-shaping assembly (BSA) system, which contains a moderator, a reflector and neutron/gamma shields, should be applied. A thermal or epithermal neutron flux (> 10^9 $n.cm^{-2}.s^{-1}$), $\dot{D}_{fast\ n}/\ \phi_{hyperthermal}$ and $\dot{D}_\gamma/\ \phi_{hyperthermal}$ (<2×10^{-13} $Gy.cm^2\ .n^{-1}$) should be measured in the BSA exit to meet the International Atomic Energy Agency (IAEA) criteria for BNCT [6].

In the present study, a 20 MeV LINAC was simulated by MCNPX Monte Carlo code in order to provide a suitable neutron flux for BNCT. After the simulations, we obtained photoneutron sources with compact sizes of 10^7,10^8 and 10^9 ($n.cm^{-2}.s^{-1}$), respectively.

2. Materials and Methods

Photoneutron yield

Photoneutron yields depend on the target material, thickness of the target material, incident electron current on the target and the geometry of photoneutron target. Therefore, photoneutron yield can be measured by the following formula [8]:

$$\text{Neutron yield } (y_n) = N_0\rho t\ \sigma_t(E)\ \varphi_e/M\ (n.s^{-1}) \quad (2)$$

where $N_0$is the Avogadro's number, M is the atomic mass, ρ is density, t denotes the thickness of the target, φ_e refers to the incident electron fluence rate (electron/s), $\sigma_t(E)$ is the total photonuclear cross-section and finally E is the incident electron energy.

The simulation of photoneutron target

In this study, MCNPX 2.6.0 Monte Carlo code was applied to simulate the transport of electrons, photons and neutrons. All these simulations were performed with a relative

error rate lower than 0.1% for 10^9 electron particles. Since the maximum energy of produced photons is 20 MeV, we used Varian 2300 C/D, which is a typical 20 MeV LINAC [11]. LINAC working values were as follows: electron current of 23 mA, electron pulse frequency of 240 Hz and pulse duration of 5 μs. In this case, the conversion factor was 1.72×10^{14} e.s^{-1}.

The first step of photoneutron target design is to produce bremsstrahlung radiation. For this purpose, LINAC was located in a 50 cm distance from (e, γ) target, and photoneutron converters and heavy elements were used. According to figure 1, uranium (U) and tungsten (W) had higher photoneutron yields than lighter elements (e.g., carbon, aluminium and nickel). Also, the maximum photoneutron yield for W converter was achieved when the thickness of W target was between 0.2 and 0.3 cm. The bremsstrahlung photon spectra were almost independent of the thickness of the target [11, 12].

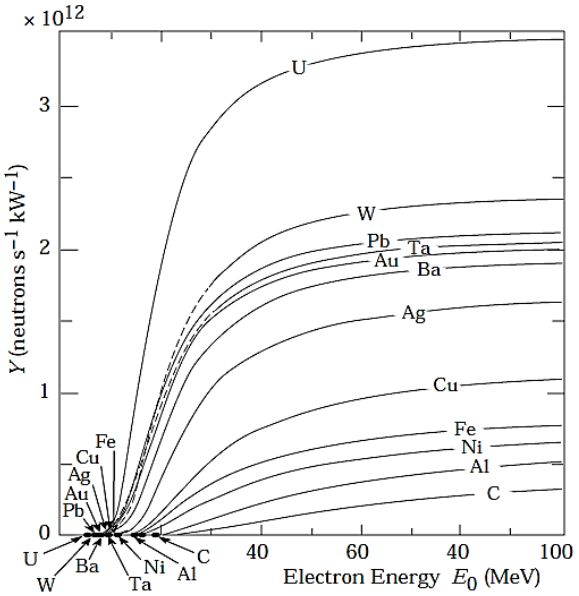

Figure 1. Neutron yields from infinitely thick targets per kW of electron beam power as a function of electron beam energy (E0), regardless of the target self-shielding [13]

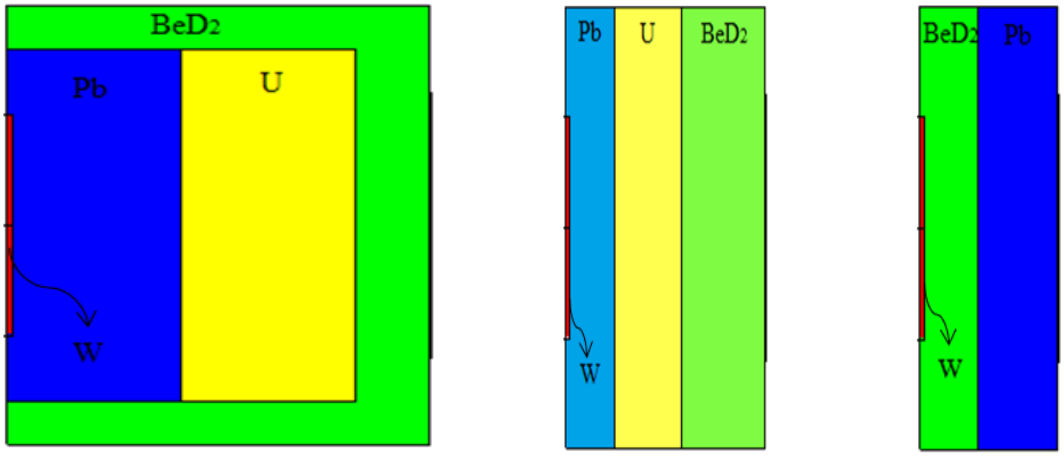

(a) (b) (c)

Figure 2. The geometry of optimized photoneutron sources, listed in table 1: a) source No. 5, b) source No. 11, c) source No. 13

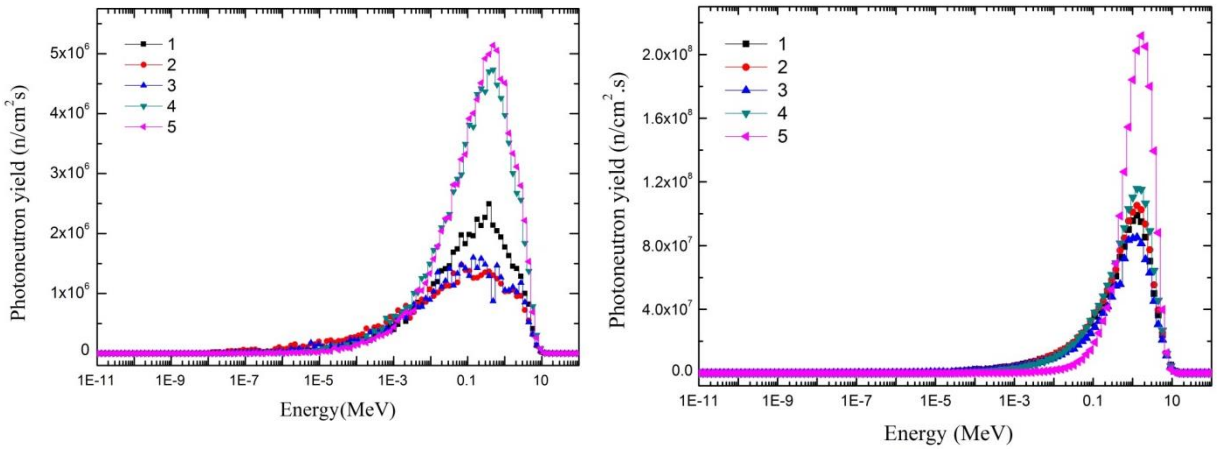

(a) (b)

Figure 3. Photoneutron yields for sources No. 1 to 5, listed in table 1: a) in front of the target with 10^7(n.cm^{-2}.s^{-1}); b) behind the target with 10^9 (n.cm^{-2}.s^{-1})

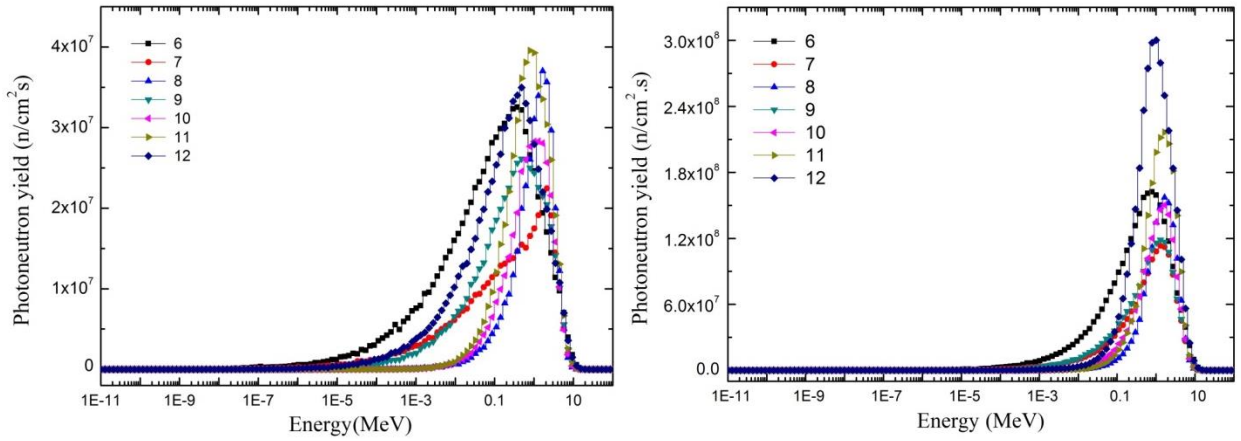

(a) (b)

Figure 4. Photoneutron yields for sources No. 6 to 12, listed in table 1: a) in front of the target with 10^8 (n.cm^{-2}.s^{-1}); b) behind the target with 10^9 (n.cm^{-2}.s^{-1})

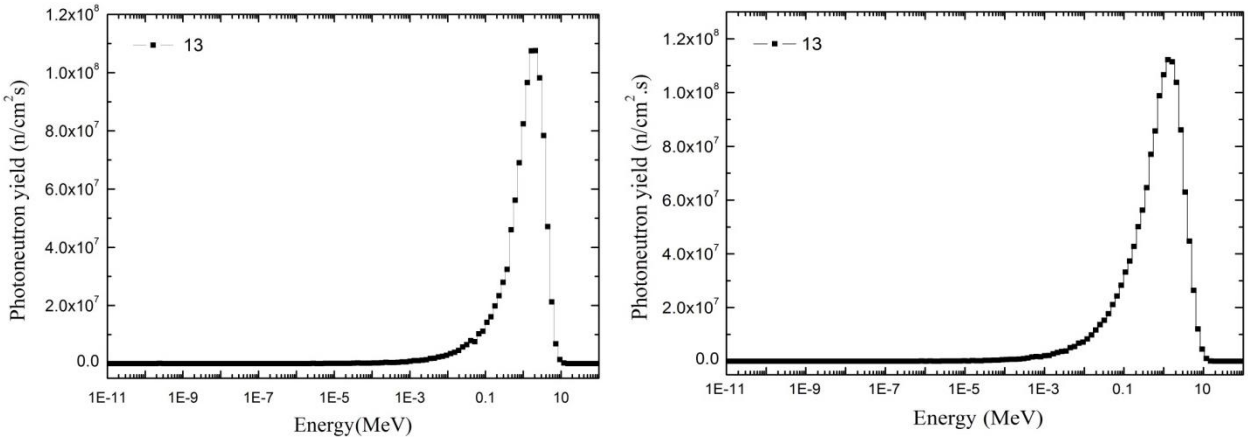

(a) (b)

Figure 5. Photoneutron yields for source No. 13, listed in table 1: a) in front of the target with 10^9 (n.cm^{-2}.s^{-1}), b) behind the target with 10^9 (n.cm^{-2}.s^{-1})

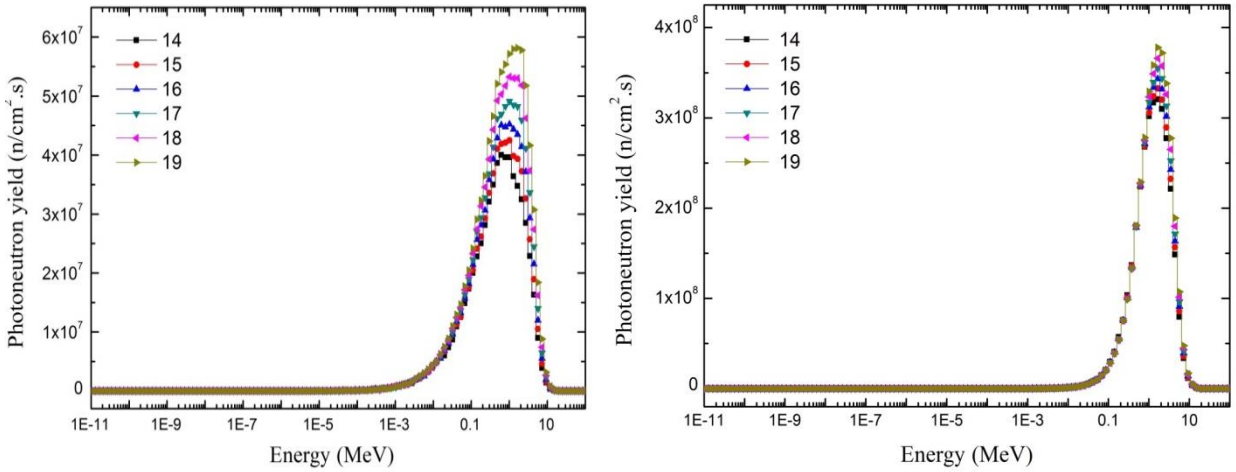

(a) (b)

Figure 6. Photoneutron yields for enriched U: (a) in front of the target with 10^8 (n/cm^2.s); b) behind the target with 10^9 (n.cm^{-2}.s^{-1})

In the present study, we used the findings of previous research. Tungsten with 0.26 cm thickness and 5 cm radius was selected as the (e, γ) converter [12]. After studying the threshold energy and material cross-sections, natural lead (Pb), U and beryllium deuteride (BeD_2) were selected as photoneutron converters with different thicknesses and radiuses. This selection optimized the photoneutron sources, as shown in table 1 (No. 5, 11 and 13 in the table denote Pb, U and BeD_2, respectively).

3. Results

In this study, Pb, U and BeD_2 were used in different compositions with a cylindrical geometry, different thicknesses and variable radiuses in front of the target. U and Pb produced more neutrons, given the high (γ, n) cross-section value. Moreover, BeD_2 could produce considerable neutrons due to lower (γ, n) threshold energy (~ 8 MeV for Pb and U and 1.67 and 2.23 MeV for Be and D, respectively).

The results of photoneutron target simulation are shown in figures 3-5. Also, we changed W and U with enriched U (10-60%) to obtain (e, γ) and (γ, n) targets with similar sizes for the photoneutron source (No. 11 in table 1 & figure 2b). The spectra of these simulations and the obtained results are shown in figure 6 and table 2, respectively.

Table 1. Photoneutron yields and average energies for different material thicknesses and radiuses in front of the target

No	Material and dimension (thickness ×radius) cm	Neutron yield ($n.cm^{-2}.s^{-1}$)	Maximum neutron Yield ($n.cm^{-2}.s^{-1}$)	Average energy (MeV)
1	BeD_2(5×10)+Pb(8×10)+U(7×10)+BeD_2	5.47E+07	2.49E+06	5.73E-01
2	BeD_2(25×10)+Pb(7×8)+U(7×8)	4.47E+07	1.37E+06	4.82E-01
3	BeD_2(26×10)+Pb(7.5×6)+U(7.5×6)	4.36E+07	1.48E+06	5.29E-01
4	BeD_2(20×10)+Pb(7×8)+U(7×8)	9.54E+07	4.73E+06	6.48E-01
5	BeD_2(17×10)+Pb(7×8)+U(7×8)	9.72E+07	5.14E+06	6.88E-01
6	BeD_2(3×10)+U(4×10)+BeD_2(5×10)	7.96E+08	3.25E+07	5.58E-01
7	BeD_2(3×10)+Pb(4×10)+BeD_2(5×10)	4.16E+08	2.24E+07	9.05E-01
8	BeD_2(9×12)+Pb(7×10)	3.53E+08	3.70E+07	1.47E+00
9	BeD_2(3×10)+Pb(3×10)+U(3×10)+BeD_2(3×10)	5.10E+08	2.61E+07	8.27E-01
10	BeD_2(2×10)+Pb(6×10)+U(2×10)+BeD_2(2×10)	3.55E+08	2.83E+07	1.25E+00
11	Pb(4×10)+U(3×10)+BeD_2(2×10)	4.89E+08	3.96E+07	1.17E+00
12	Pb(1×10)+U(4×10)+BeD_2(4×10)	6.74E+08	3.50E+07	7.10E-01
13	BeD_2(3×10)+Pb(4×10)	1.03E+09	1.07E+08	1.65E+00

Table 2. Photoneutron yields and average energies for enriched U in front of the target

No	Enriched U (%)	Neutron yield ($n.cm^{-2}.s^{-1}$)	Maximum neutron Yield ($n.cm^{-2}.s^{-1}$)	Average energy (MeV)
14	10	6.18E+08	4.00E+07	1.07E+00
15	20	6.63E+08	4.25E+07	1.12E+00
16	30	7.13E+08	4.52E+07	1.17E+00
17	40	7.66E+08	4.91E+07	1.21E+00
18	50	8.25E+08	5.32E+07	1.25E+00
19	60	8.88E+08	5.81E+07	1.29E+00

4. Discussion

The simulation results showed that the optimized photoneutron fluxes, based on forward scattering, were 10^7, 10^8 and 10^9 ($n.cm^{-2}.s^{-1}$) for photoneutron source No. 5 in figure 3a, photoneutron source No. 11 in figure 4a and photoneutron source No. 13 in figure 5a, respectively. The neutron spectrum extended from 0.001 eV to 5 MeV for source No. 5, from 0.01 eV to 5 MeV for source No. 11 and from 0.1 eV to 5 MeV for source No. 13, as shown in figures 3a-5a. The geometries of sources No. 5, 11 and 13 are shown in figure 2.

After reviewing the results, source No. 11 with neutron production of 10^8 ($n.cm^{-2}.s^{-1}$) was selected as the best photoneutron source, since its flux was higher than that of photoneutron source No. 5 (10^7 $n.cm^{-2}.s^{-1}$). In addition to higher neutron production, lower energy was of great significance due to easier neutron moderation by the BSA system. Therefore, as expected, source No. 11 was obtained approximately in the region of fast neutrons

with a rather low average energy (1.17E+00 MeV), while the average energy of photoneutron source No. 13 (1.65E+00MeV) (10^9 n.cm^{-2}.s^{-1}) was higher than that of source No. 11.

Capture cross-section value of ^{238}U for neutrons with energies higher than 1 MeV is higher than ^{208}Pb (1 >10^{-3} barn) [6]; therefore, by using U after Pb, neutrons with energies greater than 1 MeV are absorbed. Also, the elastic scattering cross-sections of Be and D are higher than absorption cross-sections; consequently, BeD_2 can be used as a moderator in the design of photoneutron sources. Also, in composite materials, regularity in locating the materials is of great significance.

Changing W and U with enriched U (10-60%) for source No. 11 could increase photoneutron yield from 6.18E+08 to 8.88E+08 (as shown in figure 6 and table 2), since photoneutron cross-section of ^{235}U was greater than ^{238}U [6]. Back scattering (scattering at θ=180°) for optimized photoneutron sources (10^9 n.cm^{-2}.s^{-1}) could be relocated in front of sources when these sources were surrounded by a moderator, a reflector and neutron/gamma shields (as shown in figures 3b-5b).

A photoneutron source, with extended energy from 0.001 eV to 5 MeV, surrounded by a BSA system, was suggested for experimental studies on the treatment of superficial cancers (e.g., skin melanoma), using BNCT. The reported results showed an obtained neutron flux of 10^7 n.cm^{-2}.s^{-1} with Pb and Be (with cylindrical geometry), which can be used for the treatment of skin melanoma [12]. The comparison of the results showed that optimized photoneutron sources, obtained from the simulations, can be used for BNCT by decelerating fast neutrons or using a suitable BSA system.

5. Conclusion

In this study, we optimized photoneutron sources with a compact volume, which can be useful for BNCT. In the simulations, we used MCNPX 2.6.0 Monte Carlo code and a 20 MeV LINAC. After studying the threshold energies and material cross-sections, Pb, U and BeD_2 were selected as photoneutron targets. Therefore, we obtained photoneutron sources with neutron production of 10^7, 10^8 and 10^9 (n.cm^{-2}.s^{-1}) for BeD_2, Pb and U composites, respectively. According to the results, in order to obtain a suitable neutron beam for BNCT, an appropriate BSA system should be designed to meet the IAEA criteria.

Acknowledgments

We would like to thank Dr. Faezeh Rahmani, Dr. Somayeh Asadi, Dr. Fatemeh Sadat Rasouli and Dr. Fatemeh Torabi for their great contribution and cooperation.

References

1. Barth RF. A critical assessment of boron neutron capture therapy: an overview. J Neurooncol.2003; 62(1-2): 1-5.
2. Salt C, Lennox AJ, Takagaki M, Maguire JA, Hosmanea NS, et al. Boron and gadolinium neutron capture therapy. Russ Chem Bull. 2004; 53 (9): 1871–88.
3. Coderre JA, Morris GM. The radiation biology of boron neutron capture therapy. Radiation research. 1999; 151 (1): 1–18.
4. Busse PM, Harling OK, Palmer MR, Kiger WS, Kaplan J, Kaplan I, et al. A critical examination of the results from the Harvard-MIT NCT program phase I clinical trial of neutron capture therapy for intracranial disease. J Neurooncol.2003; 62(1-2): 111-21.
5. Mishima Y. Selective thermal neutron capture therapy of cancer cells using their specific metabolic activities Kmelanoma as prototype. In: Mishima Y, editor. Cancer neutron capture therapy. Springer US; 1996: p.1-26.
6. IAEA-TECHDOC-1223,Current Status of Neutron Capture Therapy, ISSN 1011- 4289. 2001 May.

7. Auditore L, Barna RC, Pasquale DD, Italiano A, Trifiro A, Trimarchi M. Study of a 5MeV electron linac based neutron source. Nuclear Instruments and Methods in Physics Research Section B: Beam Interactions with Materials and Atoms. 2005;229(1):137-43.
8. Petwal VC, Senecha VK, Subbaiah KV, Soni HC and KotaiahS. Optimization studies of photo-neutron production in high-*Z* metallic targets using high energy electron beam for ADS and transmutation. PRAMANA, Journal of Physics. 2007 Feb; 68: 235241.
9. Followill DS, Stovall MS, Kry SF, Ibbott GS. Neutron source strength measurements for Varian, Simens, Elekta, and General Electric linear accelerators. J Appl Clin Med Phys. 2003;4(3):189-94.
10. Bevilacqua R, Giannini G, Calligaris F, Fontanarosa D, Longo F, Scian G, et al. A novel approach to BNCT with conventional radiotherapy accelerators. Nuclear Instruments and Methods in Physics Research Section A: Accelerators, Spectrometers, Detectors and Associated Equipment. 2007;572(1):231-2.
11. Rahmani. F, Shahriari. M. Hybrid photoneutron source optimization for electron accelerator-based BNCT. Nuclear Instruments and Methods in Physics Research Section A: Accelerators, Spectrometers, Detectors and Associated Equipment. 2010;618(1):48-53.
12. Pazirandeh. A, Torkamani.A,Taheri. A. Design and simulation of a neutron source based on an electron linear accelerator for BNCT of skin melanoma. Appl Radiat Isot. 2011;69(5):749-55.
13. Swanson WP. Calculation of neutron yields released by electrons incident on selected materials. Health Phys. 1978; 35(2): 353-67.